The Investigations of Command Shaping and Non-collocated PID Schemes in Hybrid Trajectory and Sway Control of a DPTOC System

[1]M.A. Ahmad and [2]Z. Mohamed

[1]Faculty of Electrical and Electronics Engineering, Universiti Malaysia Pahang, 26600, Pekan, Pahang, Malaysia.
(Tel: 609-424-2070; e-mail: mashraf@ump.edu.my).
[2]Faculty of Electrical Engineering, Universiti Teknologi Malaysia, 81310 UTM Skudai, Johor, Malaysia.
(e-mail:zahar@fke.utm.my)

Abstract: This paper presents investigations into the development of hybrid control schemes for trajectory tracking and sway control of a double-pendulum-type overhead crane (DPTOC) system. A nonlinear DPTOC system is considered and the dynamic model of the system is derived using the Euler-Lagrange formulation. The proposed method, known as the Single Input Fuzzy Logic Controller (SIFLC), reduces the conventional two-input FLC (CFLC) to a single input single output (SISO) controller. The SIFLC is developed for position control of cart movement. This is then extended to incorporate input shaping and non-collocated parallel proportional-integral-derivative (PID) schemes for both hook and load sway angle suppression. The positive input shapers with the derivative effects are designed based on the properties of the system. The results of the response with the controllers are presented in time and frequency domains. The performances of control schemes are examined in terms of level of input tracking capability, sway angle reduction and time response specifications in comparison to SIFLC controller. Finally, a comparative assessment of the control techniques is discussed and presented.

Keywords*:* Double-pendulum-type-overhead-crane, sway control, trajectory tracking, single input fuzzy, non-collocated PID and input shaping.

INTRODUCTION

Various attempts in controlling cranes system based on open loop and closed-loop control system have been proposed. For example, open loop time optimal strategies were applied to the crane by many researchers (Auernig and Troger, 1987; Manson, 1992). Poor results were obtained in these studies because open-loop strategy is sensitive to the system parameters and could not compensate for the effect of wind disturbance. In other hand, feedback control which is well known to be less sensitive to disturbances and parameter variations has also been adopted for controlling the crane system. For example, PD controllers has been proposed for both position and anti-swing controls (Omar, 2003). However, the performance of the controller is not very effective in eliminating the steady state error. In addition, an adaptive control strategy has also been proposed by Yang and Yang (Yang and Yang, 2006). However, the control technique requires a nonlinear control theory which needs a complicated mathematical analysis.

The modern control approaches include fuzzy logic controller (FLC) has also been proposed for controlling the crane system by several researchers (Lee and Cho, 2001). Although those modern control methods are very promising for DPTOC applications, they require substantial computational power because of complex decision making processes. However, it is possible to take full advantages of FLC for DPTOC application if the computational time of FLC is minimized. In this paper, the Single Input Fuzzy Controller (SIFLC) is proposed. The SIFLC is a simplification of the conventional Fuzzy Controller (CFLC). It is achieved by applying the signed distance method where the input to SIFLC is only one variable known as "distance" (Choi et. al., 2000). This is in contrast to the CFLC which requires an error and the derivative (change) of the error as its inputs. The reduction in the number of inputs simplifies the rule table to one-dimensional, allowing it to be treated as a single input single output (SISO) controller. As SIFLC can be treated as SISO controller, it can be a practical controller for DPTOC system. As the objective of the controlling crane system is to transfer a load from one location to another location, the position error and the velocity of the cart will be the input of the SIFLC. However, the SIFLC is limited for position control of cart and cannot cater for sway control. To overcome this problem, two types of control schemes are proposed to the system which are input shaping and non-collocated PID schemes. The aim of both controllers is to suppress the sway of hook and load angle especially when the cart reaches the desired position. In previous research, input shaping schemes has been proposed for sway angle suppression of various types of crane system (Ahmad et. al., 2009a; Ahmad et. al., 2010). However, the proposed input shaping only limited to single sway motion. Besides, a hybrid collocated and non-collocated controller has previously been addressed for control of a gantry crane system (Ahmad et. al., 2009b). The controller design utilizes sway angle feedback through a PID control scheme and proportional-derivative

(PD) for control of cart motion. However, the non-collocated PID only designed for a single sway motion.

This paper presents investigations into the development of techniques for anti-swaying and input tracking of a DPTOC system. Control strategies based on SIFLC with input shaper controller and with combined SIFLC and non-collocated PID controllers are investigated. For non-collocated control, hook and load sway angle feedback through a parallel PIDs control configuration whereas positive input shaper is utilised as a feed-forward scheme for reducing a sway effect. A simulation environment is developed within Simulink and Matlab for evaluation of performance of the control schemes. Simulation results of the response of the DPTOC system with the controllers are presented in time and frequency domains. The performances of the control schemes are examined in terms of level of input tracking capability, swing angle reduction and time response specifications in comparison to the SIFLC control. Finally, a comparative assessment of the control techniques is presented and discussed.

MATERIALS AND METHODS

The DPTOC system with its hook and load considered in this work is shown in Fig. 1, where *x* is the cart position, *m* is the cart mass, and m_1 and m_2 are the hook and load mass respectively. θ_1 is the hook swing angle, θ_2 is the load swing angle, l_1 and l_2 are the cable length of the hook and load, respectively, and *F* is the cart drive force. In this simulation, the hook and load can be considered as point masses.

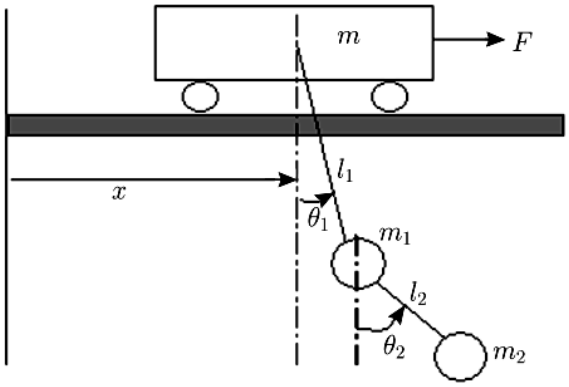

Fig. 1: Description of the DPTOC system.

This section provides a brief description on the modeling of the DPTOC system, as a basis of a simulation environment for development and assessment of the composite control techniques. The Euler-Lagrange formulation is considered in characterizing the dynamic behavior of the crane system incorporate payload.

By Lagrange's equations, the dynamic model of the DPTOC system, shown in Fig. 1, is assumed to have the following form (Spong, 1997)

$$M(q)\ddot{q} + C(q,\dot{q})\dot{q} + G(q) = \bar{\tau} \quad (1)$$

where the matrices $M(q) \in \Re^{3\times3}$, $C(q,\dot{q}) \in \Re^{3\times3}$, and $G(q) \in \Re^{3}$ represent the inertia, Centrifugal-Coriolis terms, and gravity, respectively, and are defined as

$$M(q) = \begin{bmatrix} m+m_1+m_2 & (m_1+m_2)l_1\cos\theta_1 & m_2 l_2\cos\theta_2 \\ (m_1+m_2)l_1\cos\theta_1 & (m_1+m_2)l_1^2 & m_2 l_1 l_2\cos(\theta_1-\theta_2) \\ m_2 l_2\cos\theta_2 & m_2 l_1 l_2\cos(\theta_1-\theta_2) & m_2 l_2^2 \end{bmatrix} \quad (2)$$

$$C(q,\dot{q}) = \begin{bmatrix} 0 & -(m_1+m_2)l_1\dot{\theta}_1\sin\theta_1 & -m_2 l_2\dot{\theta}_2\sin\theta_2 \\ 0 & 0 & m_2 l_1 l_2\dot{\theta}_1\sin(\theta_1-\theta_2) \\ 0 & -m_2 l_1 l_2\dot{\theta}_1\sin(\theta_1-\theta_2) & 0 \end{bmatrix} \quad (3)$$

$$G(q) = \begin{bmatrix} 0 & (m_1+m_2)gl_1\sin\theta_1 & m_2 g l_2\sin\theta_2 \end{bmatrix}^T \quad (4)$$

where *g* is the gravity effect. The state vector *q* and the control vector $\bar{\tau}$, are defined as

$$q = \begin{bmatrix} x & \theta_1 & \theta_2 \end{bmatrix}^T$$
$$\bar{\tau} = \begin{bmatrix} F & 0 & 0 \end{bmatrix}^T$$

After rearranging (1) and multiplying both sides by M^{-1}, one obtains

$$\ddot{q} = M^{-1}(-C\dot{q} - G + \bar{\tau}) \quad (5)$$

where M^{-1} is guaranteed to exist due to $\det(M) > 0$.

In this study the values of the parameters are defined as m=5 kg, m_1=2 kg, m_2=5 kg, l_1=2 m, l_2=1 m and g=9.8 m-s^{-2} (Liu et. al., 2006).

In this study, control schemes for rigid body motion control of the cart and swaying angle reduction of double pendulum are proposed. Initially, the SIFLC controller is designed. Then an input shaper and non-collocated PID control are incorporated in the closed-loop system for control of both hook and load sway angle.

Fuzzy Logic controller (FLC) is a linguistic-based controller that tries to emulate the way human thinking in solving a particular problem by means of rule inferences. Typically, a FLC has two controlled inputs, namely error (e) and the change of error ($\dot{e}$). Its rule table can be created on a two-dimensional space of the phase-plane ($e, \dot{e}$) as shown in Table 1. It is common for the rule table to have the same output membership in a diagonal direction. Additionally, each point on the particular diagonal lines has a magnitude that is proportional to the distance from its main diagonal line L_Z. This is known as the Toeplitz structure. The Toeplitz property is true for all FLC types which use the error

and its derivative terms, namely $\dot{e}, \ddot{e} \ldots$ and $e^{(n-1)}$ as input variables (Ayob et. al., 2009).

Table 1: Rule Table with Toeplitz Structure

$\dot{e}$ \ e	PL	PM	PS	Z	NS	NM	NL
NL	Z	NS	NM	NL	NL	NL	NL
NM	PS	Z	NS	NM	NL	NL	NL
NS	PM	PS	Z	NS	NM	NL	NL
Z	PL	PM	PS	Z	NS	NM	NL
PS	PL	PL	PM	PS	Z	NS	NM
PM	PL	PL	PL	PM	PS	Z	NS
PL	PL	PL	PL	PL	PM	PS	Z

By observing the consistent patterns of the output memberships in Table 1, there is an opportunity to simplify the table considerably. Instead of using two-variable input sets ($e, \dot{e}$), it is possible to obtain the corresponding output, u_0 using a single variable input only. The significance of the reduction was first realised by Choi et al. and is known as the signed distance method (Choi et. al., 2000). The method simplifies the number of inputs into a single input variable known as distance, *d*. The distance represents the absolute distance magnitude of the parallel diagonal lines (in which the input set of e and $\dot{e}$ lies) from the main diagonal line L_Z. To derive the distance, *d* variable, let $Q(e_0, \dot{e}_0)$ be an intersection point of the main diagonal line and the line perpendicular to it from a known operating point $P(e_1, \dot{e}_1)$, as illustrated in Fig. 2.

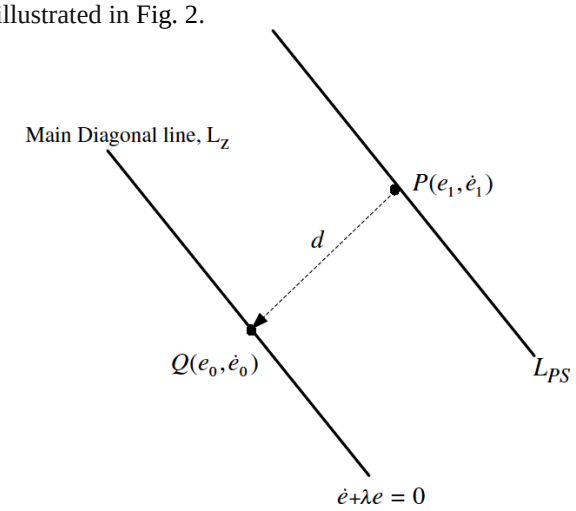

Fig. 2: Derivation of distance variable.

It can be noted that the main diagonal line can be represented as a straight line function, i.e.:

$$\dot{e} + \lambda e = 0 \tag{6}$$

In equation (6), variable λ is the slope magnitude of the main diagonal line L_Z. The distance d from point P $(e_1, \dot{e}_1)$ to point $Q(e_0, \dot{e}_0)$, can be obtained as (Ayob et. al., 2009):

$$d = \frac{\dot{e} + \lambda e}{\sqrt{1+\lambda^2}} \tag{7}$$

The derivation of distance input variable resulted in a one-dimensional rule table, in contrast to a two-dimension table required by the conventional FLC. The reduced rule table is depicted in Table 2, where L_{NL}, L_{NM} L_{NS}, L_Z, L_{PS} L_{PM} and L_{PL} are the diagonal lines of Table 2. The diagonal lines correspond to the new input of this rule table, while NL, NM, NS, Z, PS, PM and PL represent the output of corresponding diagonal lines. As can be realized, the control action of FLC is now exclusively determined by *d*. It is therefore appropriate to called it the Single Input FLC (SIFLC).

The overall structure of SIFLC, derived from the signed distance method can be depicted as a block diagram in Fig. 3. Two system state variables e (position error) and $\dot{x}$ (velocity of the cart) are selected as the feedback signal. The input to the FLC block is the distance variable *d*, while the output from FLC block is the change of control output $\dot{u}_0$. The final output of this FLC is obtained by multiplying $\dot{u}_0$ with the output scaling factor, denoted as *r*. The output equation can be written as:

$$u = \dot{u}_0 r \tag{8}$$

Accordingly, the slope magnitude, λ and output scaling factor, *r* for cart trajectory tracking were deduced as -1 and 56.03 respectively.

Table 2: The Reduced Rule Table using The Signed Distance Method

d	L_{NL}	L_{NM}	L_{NS}	L_Z	L_{PS}	L_{PM}	L_{PL}
u_0	NL	NM	NS	Z	PS	PM	PL

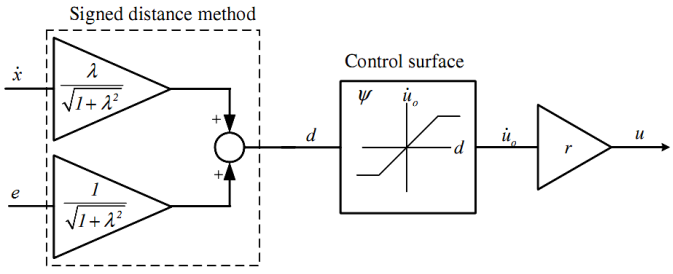

Fig. 3: SIFLC structure for DPTOC with linear control surface.

Next, the designed SIFLC is combined with input shaping scheme for control of rigid body motion of the cart and swaying angle reduction of the system. A block diagram of SIFLC with input shaping is shown in Fig. 4. Input shaping technique is a feed-forward control technique that involves convolving a desired command with a sequence of impulses known as input shaper. The shaped command that results from the convolution is then used to drive the system. Design objectives are to determine the amplitude and time locations of the impulses, so that the shaped command reduces the detrimental effects of system flexibility. These

parameters are obtained from the natural frequencies of hook and load sway angle and damping ratios of the system.

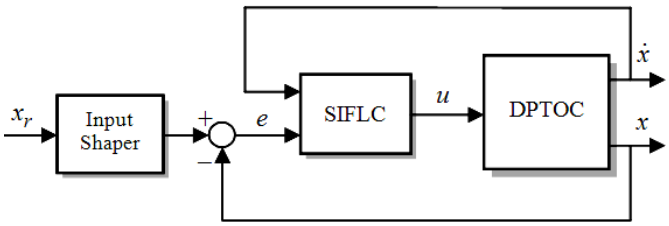

Fig. 4: SIFLC with input shaping control structure.

For the case of positive amplitudes, each individual impulse must be less than one to satisfy the unity magnitude constraint. In order to increase the robustness of the input shaper to errors in natural frequencies, the positive Zero-Sway-Derivative-Derivative (ZSDD) input shaper, is designed by solving the derivatives of the system sway equation. This yields a four-impulse sequence with parameter as

$$t_1 = 0,\ t_2 = \frac{\pi}{\omega_d},\ t_3 = \frac{2\pi}{\omega_d},\ t_4 = \frac{3\pi}{\omega_d}$$

$$A_1 = \frac{1}{1+3K+3K^2+K^3},\ A_2 = \frac{3K}{1+3K+3K^2+K^3}$$

$$A_3 = \frac{3K^2}{1+3K+3K^2+K^3},\ A_4 = \frac{K^3}{1+3K+3K^2+K^3} \qquad (9)$$

where

$$K = e^{-\zeta\pi/\sqrt{1-\zeta^2}},\quad \omega_d = \omega_n\sqrt{1-\zeta^2}$$

(ω_n and ζ representing the natural frequency and damping ratio respectively) and t_j and A_j are the time location and amplitude of impulse j respectively. The selection of natural frequency modes is very crucial in the performance of sway reduction.

Next combination is SIFLC with non-collocated PID control scheme. The non-collocated PID control scheme is connected to closed-loop configuration in parallel form for hook and load sway angle control of the system. The use of a parallel non-collocated control system, where the hook and load swing angle of the pendulum is controlled, can be applied to improve the overall performance, as more reliable output measurement is obtained. The control structure comprises three feedback loops: (1) The cart position feedback as input to compensate the control gain in SIFLC for rigid body motion control. (2) The hook swing angle of pendulum as input to a separate non-collocated PID. (3) The load swing angle of pendulum as input to a separate non-collocated PID. Both feedback loops (2) and (3) are connected in parallel using two PIDs for sway angle suppression. A block diagram of the hybrid control scheme is shown in Fig. 5 where θ_1 represents the hook swing angle of the pendulum, θ_2 represents the load swing angle of the pendulum. The control objective of both PIDs is to have zero swing angles during movement of the overhead crane.

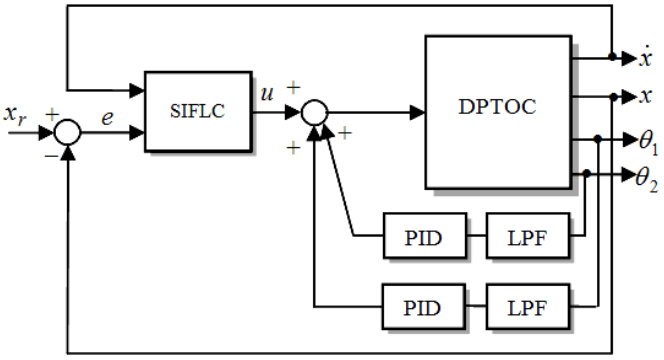

Fig. 5: SIFLC with non-collocated PID control structure.

For rigid body motion control, the SIFLC control strategy developed in the previous section is adopted whereas for the hook and load sway angle control loops, the swing angles of the pendulum feedback through a parallel PID control scheme is utilized. The PID controllers are designed and optimized by using the *Signal Constraint* block of Simulink. In order to suppress the hook and load swing angle quickly, the PID controllers are optimized based on the following desired settling time and swing amplitude of less than 10 s and 0.2 rad respectively.

Fig. 6 shows the time response constraint for optimization of PID controllers in *Signal Constraint* block. The initial parameters for PID controllers must be specified before the *Signal Constraint* block executes the tuning and optimizing process. The initial controller parameters can be obtained either by trial and error or given as default by the *Signal Constraint* block.

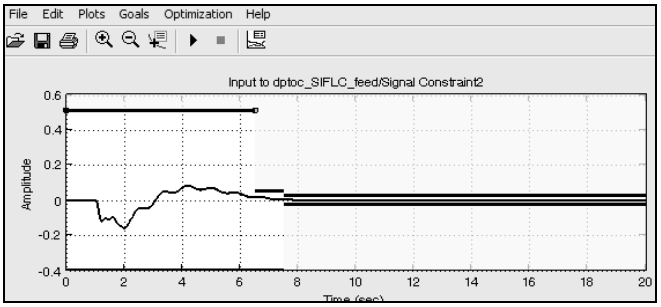

(a) Time response constraint for PID controller of hook swing angle.

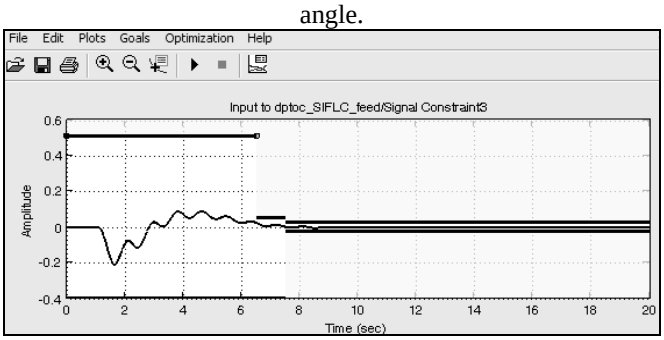

(b) Time response constraint for PID controller of load swing angle.

Fig. 6: Time response constraint for PID optimization.

Finally, the PID parameters K_p, K_i and K_d for hook swing angle suppression were deduced as 671.99, 528.21 and 204.15 respectively while for load swing angle, the parameters K_p, K_i and K_d were deduced as 19.96, 3.62×10^{-4} and 115.68 respectively. To decouple both hook and load swing angle measurement from the rigid body motion of the overhead crane's cart, a third-order infinite impulse response (IIR) Butterworth Low-pass filter was utilised. In this investigation, a Low-pass filter with cut-off frequency of 5 Hz was designed.

RESULTS AND DISCUSSION

The proposed control schemes are implemented and tested within the simulation environment of the double-pendulum-type overhead crane and the corresponding results are presented in this section. The cart of the DPTOC system is required to follow a trajectory of 5 m. System responses namely the horizontal position of the cart, hook and load swing angle of the pendulum are observed. To investigate the swing angle effect in the frequency domain, power spectral density (PSD) of the swing angle response is obtained. The performances of the control schemes are assessed in terms of sway angle suppression, input tracking capability and time response specifications. Finally, a comparative assessment of the performance of the control schemes is presented and discussed.

Figs. 7-9 show the responses of the DPTOC system to the reference input trajectory using single input fuzzy logic controller in time-domain and frequency domain (PSD). These results were considered as the system response under rigid body motion control and will be used to evaluate the performance of the input shaping and non-collocated parallel PID control. The steady-state cart position trajectory of 5 m for the DPTOC system was achieved within the rise and settling times and overshoot of 1.584 s, 8.906 s and 7.44 % respectively. It is noted that the cart reaches the required position with high overshoot and oscillation. In addition, a noticeable amount of hook and load swing angle occurs during movement of the cart. It is noted from the hook and load swing angle response with a maximum residual of ±0.6 rad and ±0.8 rad respectively. Moreover, from the PSD of the hook swing angle response the swaying frequencies are dominated by the first three modes, which are obtained as 0.2943 Hz, 1.079 Hz and 1.668 Hz with magnitude of 21.03 dB, 3.50 dB and -24.82 dB respectively. Similar for the load swing angle response, the swaying frequencies are dominated by the first three modes, which are obtained as 0.2943 Hz, 1.079 Hz and 1.668 Hz with magnitude of 22.11 dB, 11.10 dB and -15.44 dB respectively.

The cart position, hook and load swing angle and power spectral density responses of the DPTOC system using SIFLC with input shaping (SIFLC-IS) and non-collocated PID (SIFLC-PID) control are shown in Figs 7-9 respectively. It is noted that the proposed control schemes are capable of reducing the system sway while maintaining the input tracking performance of the cart position. Similar cart position, hook and load swing angle and power spectral density of both hook and load swing angle responses were observed as compared to the SIFLC.

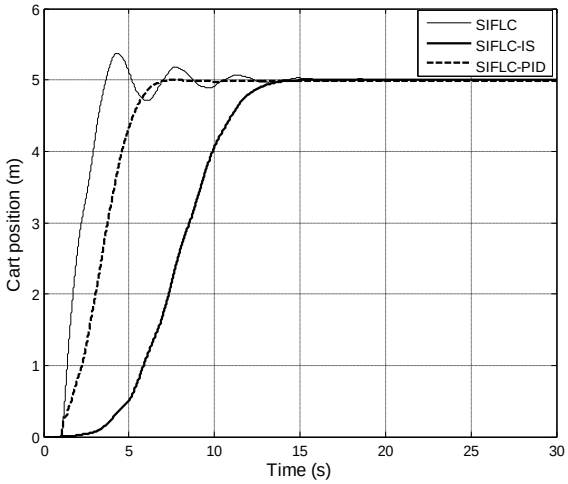

Fig. 7: Cart position response.

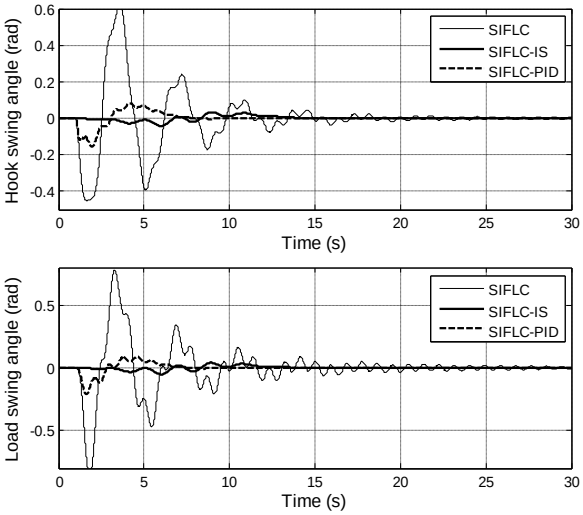

Fig. 8: Hook and load swing angle response.

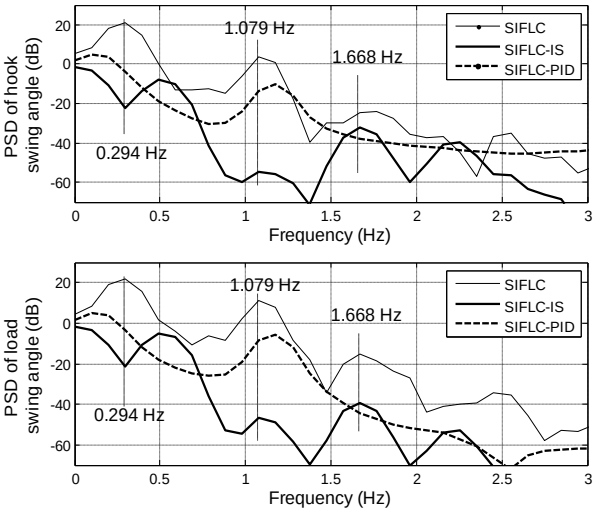

Fig. 9: PSD of hook and load swing angle response.

Table 3: Level of sway reduction of the hook and load swing angle and specifications of cart position response.

Types of controller	Swing angle	Attenuation (dB) of sway of the pendulum			Specification of cart position response		
		Mode 1	Mode 2	Mode 3	Rise time (s)	Settling time (s)	Overshoot (%)
SIFLC-IS	Hook swing angle, θ_1	43.52	58.28	7.48	6.048	10.780	0.00
	Load swing angle, θ_2	43.46	57.97	23.78			
SIFLC-PID	Hook swing angle, θ_1	24.71	17.37	13.09	3.605	5.277	0.00
	Load swing angle, θ_2	25.41	19.40	28.84			

Table 3 summarizes the levels of hook and load sway angle reduction of the system responses at the first three modes in comparison to the SIFLC control. In overall, higher levels of sway angle reduction for the first three modes were obtained using SIFLC-IS as compared to SIFLC-PID. However, the system response using SIFLC-PID is faster than the case of SIFLC-IS. It is noted with the input shaping controller, the impulses sequence in input shaper increase the delay in the system response. The corresponding rise time, setting time and overshoot of the cart position trajectory response using SIFLC-IS and SIFLC-PID is depicted in Table 3. Moreover, as demonstrated in the cart position trajectory response with SIFLC-PID control, the minimum phase behaviour of the DPTOC system is unaffected. A significant amount of hook and load swing angle amplitude suppression was demonstrated with both control schemes. With the SIFLC-PID control, the maximum amplitude of both hook and load swing angle is recorded at ±0.20 rad and the system sway settles within 9 s. However, with the SIFLC-IS control, the sway of the system settles within 13 s with a maximum residual of ±0.05 rad. Hence, it is noted that the magnitude of oscillation was significantly reduced by using SIFLC with input shaping control as compared to the case of SIFLC with non-collocated PID control. In overall, the performance of the control schemes at input tracking capability is maintained as the SIFLC control.

The simulation results show that the performance of SIFLC-IS control scheme is better than SIFLC-PID schemes in swing angle suppression of the DPTOC system. This is further evidenced in Fig. 10 that demonstrates the level of hook and load sway angle reduction at the resonance modes of the SIFLC with input shaping and non-collocated PID control respectively as compared to the SIFLC controller. It is noted that higher hook and load swing angle reduction is achieved with SIFLC-IS at the first two modes of sway angle. However, at the third modes, the differences in level of sway reduction of both cases are very small. Almost twofold and threefold improvement in the sway angle reduction at the first and second resonance mode respectively were observed with SIFLC-IS as compared to SIFLC-PID. However, as demonstrated in the cart position trajectory response, slightly slower response is obtained using SIFLC with input shaping control as compared to the SIFLC with non-collocated PID control. Further comparisons of the specifications of the cart position trajectory responses are summarized in Fig. 11 for the rise and settling times. The work thus developed and reported in this paper forms the basis of design and development of hybrid control schemes for input tracking and sway effect suppression of three-dimensional gantry crane systems and can be extended to and adopted in practical applications.

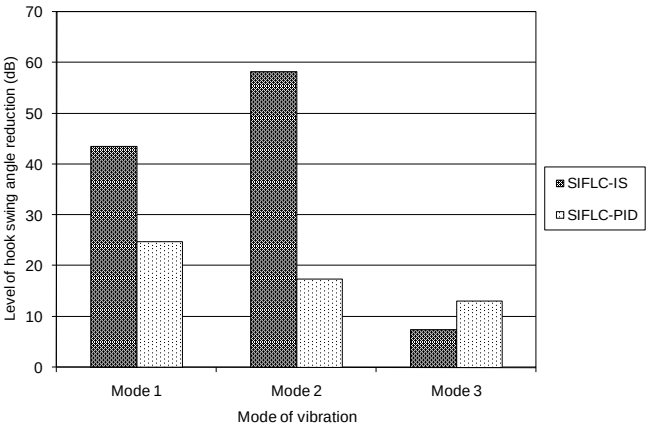

(a) Hook swing angle.

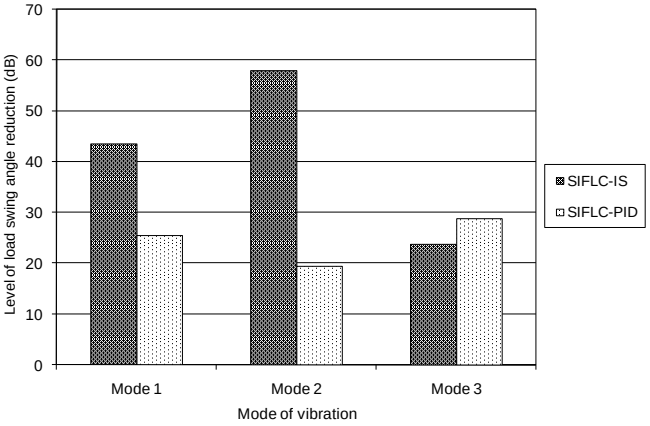

(b) Load swing angle

Fig. 10: Level of hook and load swing angle reduction.

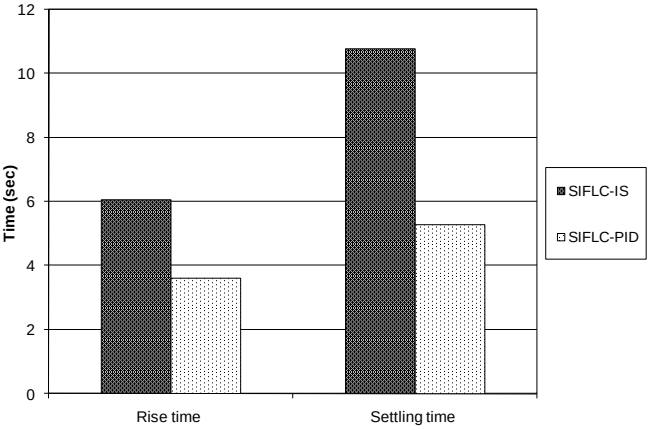

Fig. 11: Rise and settling time of cart position response.

CONCLUSION

The development of techniques for sway suppression and input tracking of the DPTOC system has been presented. The control schemes have been developed based on SIFLC with non-collocated PID control and SIFLC with input shaping technique. The proposed control schemes have been implemented and tested within simulation environment of a non-linear DPTOC system. The performances of the control schemes have been evaluated in terms of residual hook and load sway angle suppression and input tracking capability at the resonance modes of the DPTOC system. Acceptable performance in sway angle suppression and input tracking control has been achieved with proposed control strategies. A comparative assessment of the control schemes has shown that the SIFLC control with input shaping performs better than the SIFLC with non-collocated PID control in respect of swing angle reduction of both hook and load. However, the speed of the response is slightly improved at the expenses of decrease in the level of swing angle reduction by using the SIFLC with non-collocated PID control. It is concluded that the proposed controllers are capable of reducing the system sway effect while maintaining the input tracking performance of the DPTOC system.

ACKNOWLEDGEMENT

This work was supported by Faculty of Electrical & Electronics Engineering, Universiti Malaysia Pahang, especially Control & Instrumentation (COINS) Research Group and Ministry of Science, Technology and Innovation (MOSTI) under Fundamental Research Grant Scheme RDU100102

REFERENCES

Ahmad, M.A. Zulkifely, Z. Zawawi, M.A. (2010). Experimental Investigations of Input Shaping Schemes for Sway Control of a Gantry Crane System. *Proceedings of the 2nd International Conference on Computer and Network Technology*, Bangkok, Thailand, 483-486.

Ahmad, M.A., Raja Ismail, R.M.T., Ramli, M.S., Zakaria, N.F., Abd. Ghani, N.M. (2009a). Robust Feed-Forward Schemes for Anti-sway Control of Rotary Crane. *International Conference on Computational Intelligence, Modelling and Simulation*, Republic Czech, September, 17 - 22.

Ahmad, M.A., Nasir, A.N.K., and Ishak, H. (2009b). Techniques of Anti-sway and Input Tracking Control of a Gantry Crane System. *Proceedings of the 2009 IEEE International Conference on Mechatronics and Automation*, Changchun, China, 262-267.

Auernig, J. and Troger, H. (1987). Time Optimal Control of Overhead Cranes with Hoisting of the Load. *Automatica*, vol. 23(4), 437-447.

Ayob, S.M., Azli, N.A., Salam, Z. (2009). PWM DC-AC converter regulation using a multi-loop single input fuzzy PI controller. *J. Power Electron*. vol. 9(1), 124–131.

Choi, B.J., Kwak, S.W., Kim, B.K. (2000). Design and stability analysis of single-input fuzzy logic controller. *IEEE Trans. Syst. Man Cybern*., Part B, Cybern. vol. 30(2), 303–309.

Lee, H.H. and Cho, S.K. (2001). A New fuzzy logic anti-swing control for industrial three-dimensional overhead crane. *Proceedings of the 2001 IEEE International Conference on Robotic and Automation*, Seoul, 2958-2961.

Liu, D.T., Guo, W.P., and Yi, J.Q. (2006). Dynamics and Stable Control for a Class of Underactuated Mechanical Systems. *Acta Automatica Sinica*, vol. 32(3), 422-427.

Manson, G.A. (1992). Time-Optimal Control of and Overhead Crane Model. *Optimal Control Applications & Methods*, vol. 3(2), 115-120.

Omar, H.M. (2003). Control of Gantry and Tower Cranes, M.S. Thesis, Virginia Tech., Blacksburg, VA.

Spong, M.W. (1997). Underactuated Mechanical Systems, Control Problems in Robotics and Automation. London: Springer-Verlag.

Yang, J.H. and Yang, K.H. (2006). Adaptive coupling control for overhead crane systems. Available from: http://www.sciencedirect.com, Accessed : 2006-12-24.